

with size, the NOESY maps can be expected to be particularly informative for the larger paramagnetic metalloproteins, such as hemerythrins,<sup>26</sup> uteroferrins,<sup>27</sup> and various superoxide dismutase complexes.<sup>28</sup>

**Acknowledgment.** This research was supported by a grant from the National Institutes of Health, GM 26226. The GE  $\Omega$ -300 NMR spectrometer was purchased in part with funds provided by a grant from the National Science Foundation, DIR-90-16484.

(28) Banci, L.; Bencini, A.; Bertini, I.; Luchinat, C.; Piccioli, M. *Inorg. Chem.* 1990, 29, 4867 and references therein.

## Slow Conformational Dynamics at the Metal Coordination Site of a Zinc Finger

G. Marius Clore,\* James G. Omichinski, and Angela M. Gronenborn\*

Laboratory of Chemical Physics, Building 2  
National Institute of Diabetes and Digestive and  
Kidney Diseases, National Institutes of Health  
Bethesda, Maryland 20892

Received January 15, 1991

We recently described the determination of the high-resolution three-dimensional structure of a synthetic 30-residue classical Cys<sub>2</sub>His<sub>2</sub> zinc finger domain of the human enhancer binding protein in solution by NMR.<sup>1</sup> This communication extends this work to include an investigation of dynamical properties and presents direct evidence for slow conformational exchange between several species involving the histidine side chains coordinated to the zinc atom.

Figure 1 shows homonuclear Hartmann-Hahn (HOHAHA)<sup>2</sup> and nuclear Overhauser enhancement (NOESY)<sup>3</sup> spectra comprising the region of the C<sup>1</sup>H resonances of the histidine residues of 4.8 mM peptide in the presence of a molar excess of ZnCl<sub>2</sub> at pH 5.8 and 6 °C. Of the three histidine residues present in this zinc finger, the two that are liganded to zinc, His-21 and His-27, exhibit three sets of resonances, one at 7.33 and 7.75 ppm, respectively, corresponding to a major form (A), and two sets ~0.25 ppm to lower field corresponding to two minor forms (B and C). Cross peaks between these sets of resonances (labeled C,A and B,A) are seen in both the NOESY and HOHAHA spectra. As the sign of these cross peaks in the spin-locked HOHAHA spectrum is the same as that of the diagonal, and as these minor resonances do not correspond to the C<sup>2</sup>H protons of histidine, they must arise through chemical exchange.<sup>4</sup> A similar set of exchange cross peaks is also seen for the C<sup>2</sup>H proton of His-27 where the chemical shifts of the two minor forms are degenerate and ~0.39 ppm downfield of that observed for the major species. No exchange peaks were observed for the C<sup>2</sup>H proton of His-21. In addition, a number of other resonances of residues in close spatial proximity to the histidine residues also appear to exhibit exchange cross peaks, but as the chemical shift differences are smaller and they occur in crowded regions of the spectrum, they are difficult to assign

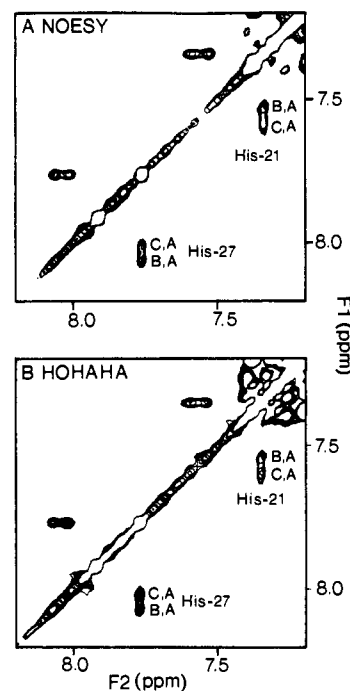


**Figure 1.** Histidine C<sup>1</sup>H region of the (A) 150-ms NOESY and (B) 36-ms HOHAHA spectra of the human enhancer zinc finger domain. The spin-lock field in the HOHAHA spectrum was generated by a WALTZ-17 mixing sequence<sup>2</sup> with a radio frequency field strength of ~8 kHz. Experimental conditions: 4.8 mM peptide, 50 mM ZnCl<sub>2</sub>, pH 5.8, 6 °C. (Note that identical results are obtained with a 1:1 ratio of peptide to zinc.)

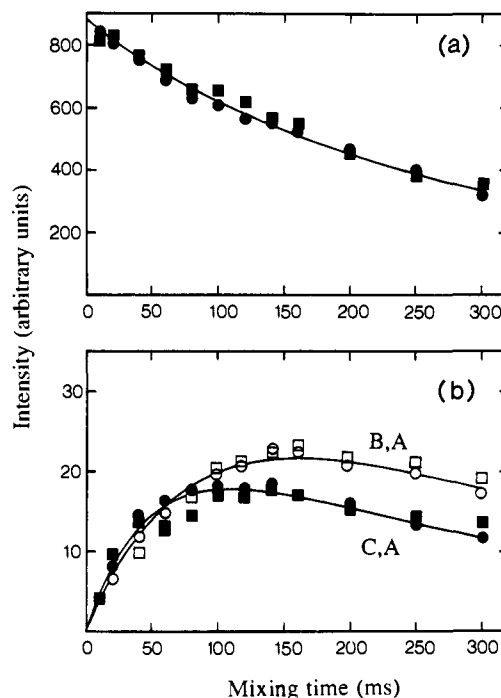


**Figure 2.** Comparison of the experimental and best fit calculated time dependences of (a) the diagonal resonances of the major species and (b) the exchange cross peaks between the major and minor species for the C<sup>1</sup>H protons of His-21 and His-27 in a series of NOESY spectra with mixing times ranging from 10 to 300 ms. The experimental data (at pH 5.8, 6 °C) for His-21 and His-27 are shown as circles and squares, respectively, while the lines represent the best fits obtained by integration of the differential equations given by eq 1. All the data were fitted simultaneously by using the program FACSIMILE.<sup>6</sup>

unambiguously. Because the population of species B and C is so small, no exchange cross peaks between B and C are observed as their expected intensity is below the limit of detection.

(1) Omichinski, J. G.; Clore, G. M.; Appella, E.; Sakaguchi, K.; Gronenborn, A. M. *Biochemistry* 1990, 29, 9324.

(2) (a) Davis, D. G.; Bax, A. *J. Am. Chem. Soc.* 1985, 107, 2821. (b) Bax, A. *Methods Enzymol.* 1989, 176, 151.

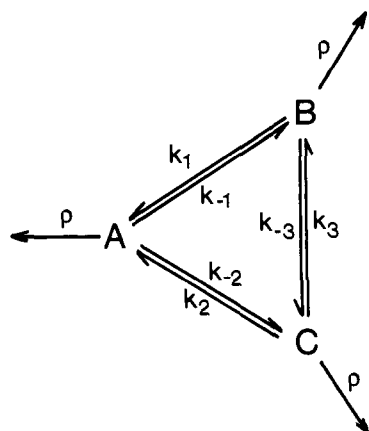
(3) (a) Jeener, J.; Meier, B. H.; Bachmann, P.; Ernst, R. R. *J. Chem. Phys.* 1979, 71, 4546. (b) Macura, S.; Huang, Y.; Suter, D.; Ernst, R. R. *J. Magn. Reson.* 1981, 43, 259.

(4) (a) Bothner-By, A. A.; Stephens, R. L.; Lee, J. T.; Warren, C. D.; Jeanloz, R. W. *J. Am. Chem. Soc.* 1984, 106, 811. (b) Bax, A.; Davis, D. G. *J. Magn. Reson.* 1985, 63, 207.

(5) McConnell, H. M. *J. Chem. Phys.* 1958, 28, 430.

(6) (a) Chance, E. M.; Curtis, A. R.; Jones, I. P.; Kirby, C. R. *U.K. At. Energy Auth., Harwell Lab.* 1979, AERE-R 8775. (b) Curtis, A. R. *U.K. At. Energy Auth., Harwell Lab.* 1979, AERE-R 9352. (c) Clore, G. M. In *Computing in Biological Science*; Geisow, M. J., Barrett, M., Eds.; Elsevier North-Holland: Amsterdam, 1983; p 313.

Scheme I



The time dependence of the exchange cross peaks and corresponding diagonal resonances in a series of NOESY spectra recorded with mixing times ranging from 10 to 300 ms at pH 5.8 is shown in Figure 2, together with the best-fit theoretical curves using the simple three-species model of Scheme I. A is the major species, B and C are the two minor species,  $k_i$  are the rate constants for interconversion between the species, and  $\rho$  is the total spin-lattice relaxation rate of the relevant proton, which for simplicity is assumed to be the same for the two histidines of all three species. The time development of magnetization in such a system is described by<sup>5</sup>

$$\begin{aligned} dM_A/dt &= -M_A(\rho + k_{-1} + k_{-2}) + M_Bk_1 + M_Ck_2 \\ dM_B/dt &= -M_B(\rho + k_1 + k_{-3}) + M_Ak_{-1} + M_Ck_3 \\ dM_C/dt &= -M_C(\rho + k_2 + k_3) + M_Ak_{-2} + M_Bk_{-3} \end{aligned} \quad (1)$$

The equilibrium constants between the species are defined as  $K_1 = k_1/k_{-1} = [A]/[B]$ ,  $K_2 = k_2/k_{-2} = [A]/[C]$ , and  $K_3 = k_3/k_{-3} = [B]/[C] = K_2/K_1$ . The intensity of a given diagonal peak and its associated cross peaks as a function of mixing time  $t$  is obtained by solving eq 1 with the magnetization of the species corresponding to the diagonal peak set to 1 in the case of the major species A (and to  $1/K_1$  or  $1/K_2$  in the case of minor species B or C) and the magnetization of all other species set to 0. The complete set of build-up curves was fitted *simultaneously* by carrying out successive numerical integration runs under control of a nonlinear least-squares optimization routine, varying the values of the rate constants  $k_1$ ,  $k_{-1}$ ,  $k_2$ ,  $k_{-2}$ , and  $\rho$ , and a scale factor. The exact values of  $k_3$  and  $k_{-3}$  have a minimal effect on the system as the equilibrium constant  $K_3$  is determined by the other two equilibrium constants, so that for simplicity  $k_{-3}$  was set to  $10^{-4} \text{ s}^{-1}$ .

The diagonal and exchange cross peaks of the two histidine residues exhibit the same time dependence, indicating that they are associated with the same dynamical processes. The results of the analysis are summarized in Table I for data collected at pH 5.8 and 7.0. At pH 5.8, 91.3% of the zinc finger is in form A, 5.3% in form B, and 3.4% in form C, and there is no significant change in these values at pH 7.0. The main difference between the data at pH 5.8 and 7.0 lies in the rates for the interconversion between species A and C, which are approximately half those at pH 5.8.

At pH values above 5.5 the equilibrium constant for the binding of zinc to the peptide is  $\geq 10^6 \text{ M}^{-1}$  so that, under the experimental conditions employed, the concentration of zinc-free peptide is  $\ll 0.01\%$  of the total peptide present. Thus, the simplest explanation for the observed exchange phenomena is one in which both histidines are liganded to zinc in species A, while in species B and C, only one of the histidine residues is liganded to the metal with the fourth coordination position either unoccupied or possibly taken by a water molecule. Examination of the structure of the zinc finger<sup>1</sup> indicates that only a small change in the  $\chi_2$  angle of the histidines is required to accomplish this. The downfield shift of the histidine resonances of the two minor forms can probably be

Table I. Equilibrium and Rate Constants for Scheme I Obtained from a Nonlinear-Least-Squares Fit to the Experimental Data at 6 °C

	pH 5.8	pH 7.0
$k_1$ ( $\text{s}^{-1}$ )	$7.8 \pm 1.1$	$6.7 \pm 0.5$
$k_{-1}$ ( $\text{s}^{-1}$ )	$0.5 \pm 0.03$	$0.4 \pm 0.03$
$k_2$ ( $\text{s}^{-1}$ )	$16.3 \pm 1.8$	$8.8 \pm 0.8$
$k_{-2}$ ( $\text{s}^{-1}$ )	$0.6 \pm 0.05$	$0.4 \pm 0.05$
$K_1$	$17.1 \pm 1.5$	$17.2 \pm 1.1$
$K_2$	$28.5 \pm 1.4$	$24.0 \pm 1.5$
$K_3$	$1.7 \pm 0.1$	$1.4 \pm 0.1$
$\rho$ ( $\text{s}^{-1}$ )	$2.9 \pm 0.2$	$2.6 \pm 0.4$

attributed to a partial net positive charge on the zinc atom arising from the change in histidine coordination and resulting in deshielding of the histidine imidazole protons.

The present data clearly indicate the presence of dynamical transitions between a major and two minor species of a zinc finger domain which occur on time scales in the millisecond to second range. Although the occupancy of these minor species is low, namely, of the order of a few percent, they are nevertheless easily observable, and any naive interpretation of the associated cross peaks may have led to incorrect conclusions.

**Note Added in Proof.** Two recent reports on zinc finger peptides (Kochoyan et al. *Biochemistry* 1991, 30, 3371; Xu et al. *Ibid.* 1991, 30, 3365) suggest the possibility of multiple conformations although no proof as exemplified by exchange cross peaks was presented.

**Acknowledgment.** We thank Drs. E. Appella and K. Sakaguchi for useful discussions. This work was supported by the AIDS Directed Anti-Viral Program of the Office of the Director of the National Institutes of Health (G.M.C. and A.M.G.).

### Ab Initio Studies of a Marginally Stable Intermediate in the Base-Catalyzed Methanolysis of Dimethyl Phosphate and Nonexistence of the Stereoelectronically Unfavorable Transition State

Tadafumi Uchimaru,\*<sup>†</sup> Kazutoshi Tanabe,<sup>†</sup>  
Satoshi Nishikawa,<sup>‡</sup> and Kazunari Taira\*<sup>‡</sup>

National Chemical Laboratory for Industry and  
Fermentation Research Institute  
Agency of Industrial Science & Technology  
MITI, Tsukuba Science City 305, Japan

Received October 16, 1990

A pentacoordinated oxyphosphorane, whose properties are not easily elucidated experimentally, is a common intermediate/transition state for the hydrolysis and transesterification of phosphate esters. RNA cleaving reactions proceed via a five-membered cyclic oxyphosphorane.<sup>1-3</sup> Previously, we carried out ab initio STO-3G studies on cyclic oxyphosphorane dianion **2a** as a model compound for the RNA cleaving process (1).<sup>4</sup> The calculations indicated that the transition state for the exocyclic P-O<sub>5</sub> bond breaking step is higher in energy than that for the endocyclic P-O<sub>2</sub> bond breaking step (rapid equilibrium). The origin of the energy difference between these two transition states is likely to be attributable to a combination of stereoelectronic

<sup>†</sup> National Chemical Laboratory for Industry.

<sup>‡</sup> Fermentation Research Institute.

(1) Breslow, R.; Labelle, M. *J. Am. Chem. Soc.* 1986, 108, 2655-2659.

(2) Anslyn, E.; Breslow, R. *J. Am. Chem. Soc.* 1989, 111, 4473-4482.

(3) Taira, K. *Bull. Chem. Soc. Jpn.* 1987, 60, 1903-1909.

(4) Taira, K.; Uebayasi, M.; Maeda, H.; Furukawa, K. *Protein Eng.* 1990, 3, 691-701.